

Modeling of Arterial Stiffness using Variations of Pulse Transit Time

Aleksandar Peulić¹, Natasa Milojević², Emil Jovanov³, Miloš Radović⁴, Igor Saveljić⁴, Nebojša Zdravković⁵, Nenad Filipović⁴

¹ Technical Faculty, University of Kragujevac, Svetog Save 65,
32000 Cacak, Serbia

² Intellectual Property Office, Kneginje Ljubice 5,
11000 Belgrade, Serbia

³ Electrical and Computer Engineering, University of Alabama,
Huntsville, AL 35899 USA

⁴ Faculty of Engineering, University of Kragujevac, Jovana Cvijica bb,
34000 Kragujevac, Serbia

⁵ Medical Faculty, University of Kragujevac, Svetozara Markovica 69,
34000 Kragujevac, Serbia

Abstract. In this paper, a finite element (FE) modeling is used to model effects of the arterial stiffness on the different signal patterns of the pulse transit time (PTT). Several different breathing patterns of the three subjects are measured with PTT signal and corresponding finite element model of the straight elastic artery is applied. The computational fluid-structure model provides arterial elastic behavior and fitting procedure was applied in order to estimate Young's module of stiffness of the artery. It was found that approximately same elastic Young's module can be fitted for specific subject with different breathing patterns which validate this methodology for possible noninvasive determination of the arterial stiffness.

Keywords: arterial stiffness, finite element modeling, microcontroller, pulse transit time.

1. Introduction

Pulse Transit Time (PTT) represents the time which blood pulse wave propagates from heart to a peripheral artery measurement site (for example, the finger). It has an important role in noninvasive assessment of blood pressure. The components of photoplethysmogram (PPG) signal are not fully understood. It is generally accepted that they can provide valuable information about the cardiovascular system [1]. PTT is measured using

electrocardiogram (ECG) and (PPG) [2]. The pulse pressure waveform is getting from the left ventricle blood ejection into the aorta. There are two main parameters of the wave pulse: the blood velocity and pulse wave velocity. The blood velocity at the aorta is several meters per second and it slows down to several mm/s in the peripheral network while the pressure pulse travels much faster than blood [3]. Pulse wave velocity (PWV) is a direct measurement of arterial stiffness and describes how quickly a blood pressure pulse travels from one point to another in the human body and the time spent for such process is the PTT [4]. The value of the PWV, is affected by several factors, such as the elasticity of arterial wall, arterial geometry (radius and thickness), and blood density. Typical value ranges from 5 m/s to 15 m/s, depending on the age of people and the state of their arteries [5].

2. Related work

Atherosclerosis is a disease that increases the thickness and rigidity of the arterial blood vessels, causing narrowing of artery. The increased inflexibility of the arterial wall increases PWV, since the energy of the blood pressure pulse cannot be stored in an inflexible wall. PWV can be used as a predictor of cardiovascular mortality in hypertensive subjects [6].

In a number of other studies [7], [8], [9], [10], when comparing the results of the analysis of heart rate variability and pulse rate variability, some differences are revealed. That can be explained by temporal changes of hemodynamic parameters of the vascular system controlled by vascular regulation. Some authors tried to find characteristics defined in the frequency domain and the characteristics of the vascular system in order to obtain a diagnostic index of the vascular system, which may be used to estimate arterial stiffness [9], [10].

In this paper the finite element modeling of cardiovascular pulsation with combination of the PTT measurements on the finger of left hand is described, and we present experimental measurements, computational strategy and results of modeling validated by experiments. The main aim of this study was to find correlation of the arterial elastic Young's module with PTT.

3. Experimental measurements

Pulse travel time is measured as time period between contraction of the ventricles and arrival of the blood pulse to the left index finger. Contraction of the ventricles is detected using R peak of the ECG signal; arrival of the blood pulse is detected as the half rise point of PPG signal. Electrodes are connected with wires to the recording device which is sometimes connected with wires to the processing device. This configuration is not convenient to the patient and to the researches too. The wires make some movements

Modeling of Arterial Stiffness using Variations of Pulse Transit Time

difficult and they alter normal behavior of a patient. Taking this into consideration we selected elastic belt with embedded electrodes and capturing device on the belt. The capturing device sends ECG R peak signal wirelessly to the processing board. PPG sensor is attached to the finger or ear and connected to the processing board. Processing board captures ECG signal and PPG signal and determines delay between consecutive R peaks for ECG and PPG signals. For further processing it should have sufficient amount of memory, low frequency clock and timer with capture/compare registers. Processing board can display result on LCD and/or transmit the result to PC via Ethernet or serial line. The overall hardware architecture is shown in Fig. 1 and PTT timing diagram in Fig. 2.

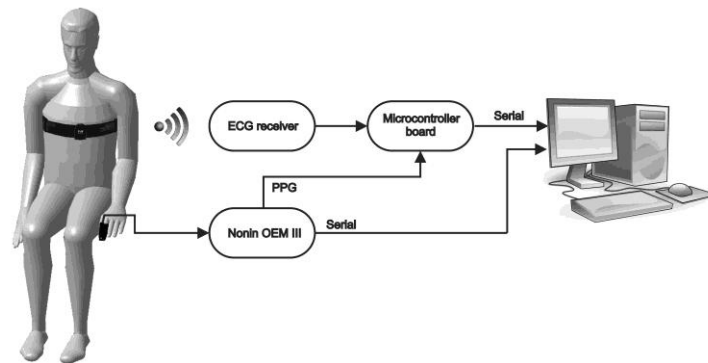


Fig. 1. Hardware architecture

Precise measurement of the PTT with minimum latency is implemented using digital output of the PPG sensor (OEM III board from Nonin [11]) and custom ECG peak capture board connected to the input pins of timer on the processing board. Timer capture/compare registers used input pin interrupts to capture relative timing of ECG and PPG signals. Measured intervals are sent to PC for display and processing. Fixed point FIR filtering routines for ECG signal are implemented in firmware, code below:

```
int filterlp(int sample)
// Lowpass FIR filter for EKG
{ static int buflp[32];
// Reserve 32 locations for circular buffering
static int offsetlp = 0;
long z;
int i;
buflp[offsetlp] = sample;
z = mull6(coeffslp[8], buflp[(offsetlp - 8) &
0x1F]);
for (i = 0; i < 8; i++)
```

Aleksandar Peulić et al.

```
        z += mul16(coeffslp[i], buf1p[(offsetlp - i) &
0x1F] + buf1p[(offsetlp - 16 + i) & 0x1F]);
        offsetlp = (offsetlp + 1) & 0x1F;
        return z >> 15;
// Return filter output
}

int filterhp(int samplehp)
// Highpass FIR filter for hear rate
{
    static int bufhp[32];
// Reserve 32 loactions for circular buffering
    static int offsethp = 0;
    long z;
    int i;
    bufhp[offsethp] = samplehp;
    z = mul16(coeffshp[8], bufhp[(offsethp - 8) &
0x1F]);
    for (i = 0; i < 8; i++)
        z += mul16(coeffshp[i], bufhp[(offsethp - i) &
0x1F] + bufhp[(offsethp - 16 + i) & 0x1F]);
    offsethp = (offsethp + 1) & 0x1F;
    return z >> 15;
// Return filter output
}
}
```

Code below represents main firmware procedure and sends the two bytes of the ADC register to the PC Application via USB interface:

```
void main(void)
{
    Init ();
// Initialize device for the application
    while(1)
    {LPM0;
// Enter LPM0 needed for UART TX completion

        Dataout = filterlp(Datain);
// Lowpass FIR filter for filtering out 60Hz
        Dataout_pulse = filterhp(Dataout)-128;
// Highpass FIR filter to filter muscle artifacts
        Dataout = Dataout >> 6;
// Scale Dataout to use PC program

        if(Dataout>255)
// Set boundary 255 max
            Dataout=255;
//
        if(Dataout<0)
// Set boundary 0 min
            Dataout=0;
//
    }
}
```

Modeling of Arterial Stiffness using Variations of Pulse Transit Time

```
    samples[0] = Dataout;
    send_data();
//sends

    counter++;
// Debounce counter
    pulseperiod++;
// Pulse period counter
    if (Dataout_pulse > 48)
// Check if above threshold
    { LCDM10 |= 0x0f;
// Heart beat detected enable "^" on LCD
    counter = 0;}
// Reset debounce counter
    if (counter == 128)
// Allow 128 sample debounce time
    {LCDM10 = 0x00;
// Disable "^" on LCD for blinking effect
    beats++;
    if (beats == 3)
    {beats = 0;
    heartrate = itobcd(92160/pulseperiod);
// Calculate 3 beat average heart rate per min
    pulseperiod = 0;
// Reset pulse period for next measurement
    LCDMEM[0] = char_gen[heartrate & 0x0f];
// Display current heart rate units
    LCDMEM[1] = char_gen[(heartrate & 0xf0) >> 4];
// tens
    LCDMEM[2] = char_gen[(heartrate & 0xf00) >> 8];}}
// hundreds
    }
}
} //main
void send_data(void)
{
    for (j=0;j<1;j++)
    {
        while (!(IFG1 & UTXIFG0));
// USART0 TX buffer ready?
        TXBUF0 = samples[j];
    }
}
```

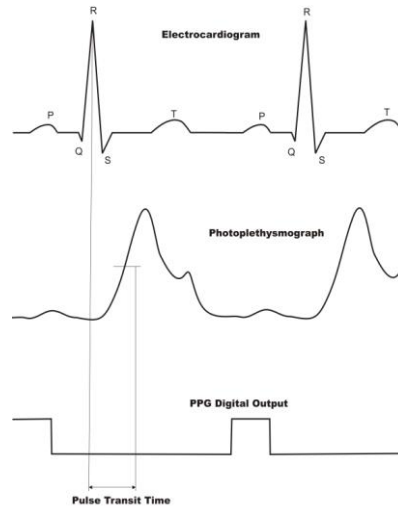


Fig. 2. PTT illustration. RR is time interval between two R peaks in the ECG

In order to validate modeling of arteries in different physiological conditions, eight breathing experiments were conducted. The goal of these experiments was to record difference in RR (RR is time interval between two R peaks in the ECG signal) and PTT measurements due to different breathing patterns and to model the changes using Finite Element (FE) modeling. The experiment was conducted in the sitting position and consisted of few steps:

Subject_1:

normal breathing: 1 minute; paced breathing at 5sec/breath for two minutes;
paced breathing at 10 sec/breath for two minutes; normal breathing 1 minute

Subject_2:

normal breathing: 5 minute; paced breathing at 5sec/breath for five minutes;

Subject_3:

normal breathing: 5 minute; paced breathing at 5sec/breath for five minutes.

PTT measurements for all subject are presented in Fig. 3 and RR measurements are given in Fig. 4.

Modeling of Arterial Stiffness using Variations of Pulse Transit Time

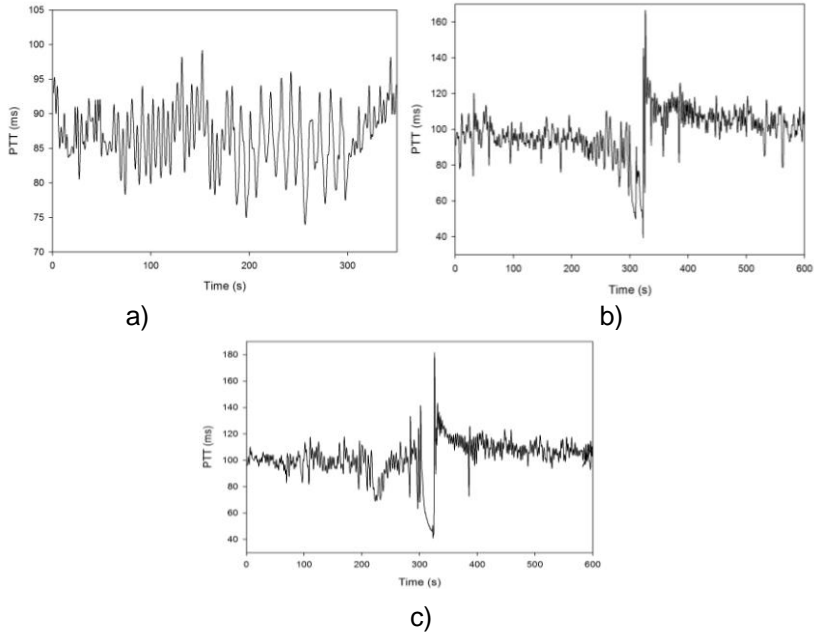


Fig. 3. PTT measurements: a) Subject_1, b) Subject_2, c) Subject_3

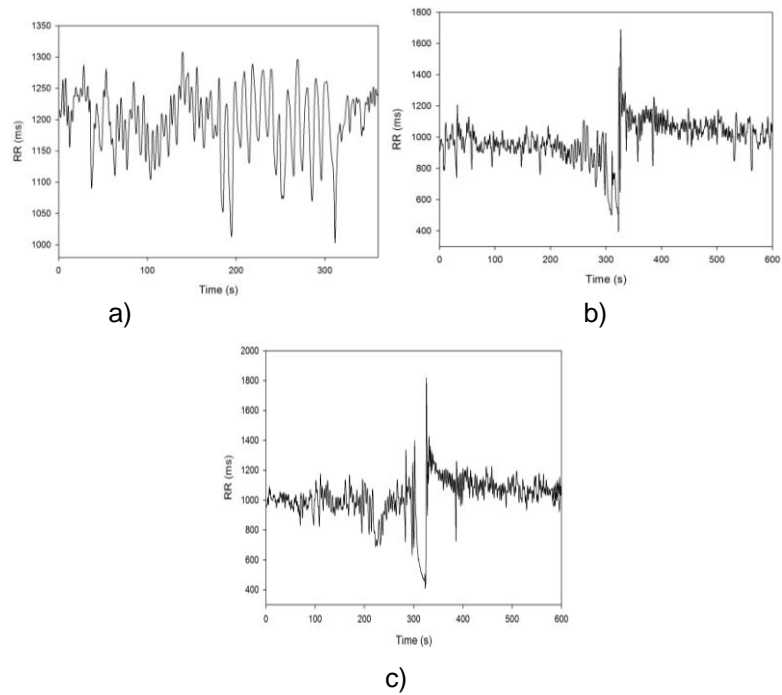


Fig. 4. RR measurements: a) Subject_1, b) Subject_2, c) Subject_3

4. Computational modeling results

Computer modeling is a useful tool for the study of dynamic behavior of blood flows in the arteries.

PWV provides an assessment of the state of the cardiovascular system. Pressure pulse velocity is determined by elastic and geometric properties of arterial wall. It can be expressed by the Bramwell-Hill equation [2]

$$PWV = \sqrt{\frac{V}{\rho} \frac{\Delta P}{\Delta V}} \quad (1)$$

where V is blood volume, ΔV and Δp are the changes of blood volume and pressure, and ρ is the density (of blood). This relation enables the study of compliance (arterial elasticity) by measuring the PWV. Also, Moens-Korteweg equation can be used to determine a PWV [2]

$$PWV = \sqrt{\frac{\Delta E h_w}{2 \rho_w r_i}} \quad (2)$$

where ΔE is the incremental elastic modulus, ρ_w is wall density, h_w is the thickness of the arterial wall and r_i is the internal vessel radius. The Bramwell-Hill Eq. (1) and the Moens-Korteweg Eq. (2) are the same equations, just with different denotation. Eq (1) is more applicable in medical technology because gives direction relation of quantities ΔV and Δp . Actually a small rise in pressure may be shown to cause a small increase, in the radius of the artery, or a small increase, in its own volume V per unit length. Both Eqs. (1) and (2) can be derived from Newton's equation for wave speed using the substitution of the equation of the bulk modulus in terms of volumetric strain. Relationship between PTT and PWV can be represented as [12]

$$PTT = \frac{L}{PWV} \quad (3)$$

where L is the distance the pulse travels (roughly equals to the aorta ascending arch plus arm length). In this paper, we simulate a blood vessel as an elastic tube where fluid flows in a periodic time function, which corresponds to the periodic heart rate. We model the straight artery of length 700 mm, lumen radius 3.8 mm and wall thickness 0.5 mm. The comparison of analytical solution from Moens-Korteweg theory (2) and numerical solutions by varying Young's modulus is shown in Fig. 5. A very good agreement of numerical solutions with analytical results is achieved, where mean difference of the two curves is 0.10 m/s, standard deviation has a value of 0.0478 m/s, while the standard error is 0.0169.

Modeling of Arterial Stiffness using Variations of Pulse Transit Time

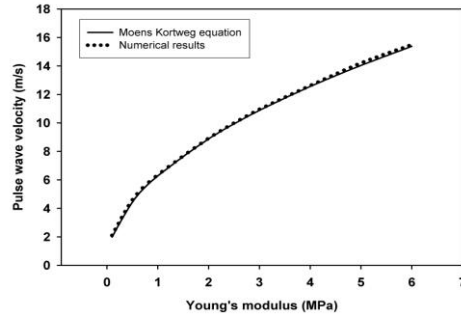


Fig. 5. Pulse wave velocity as function of incremental Young's modulus. Comparison of numerical and analytical solution

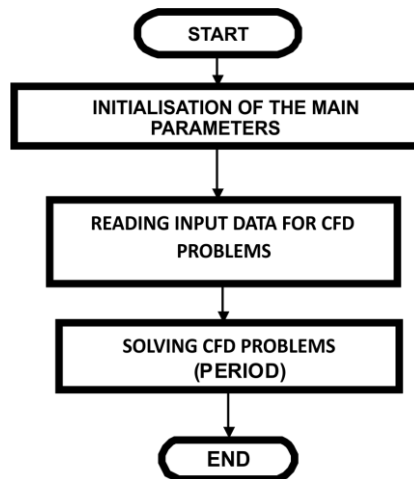


Fig. 6 Flow chart for program for finite element method for CFD

Global FLOW CHART for Program for Finite element method is presented in Fig 6. After initialization of the main parameters of the program, input data as finite element nodes and elements, boundary conditions, initial conditions, material properties, time step function are reading. Then finite element solver is running for CFD problems. The solver is un-symmetric because pressure velocity formulation. For faster calculation we implemented a penalty formulation in our solver [14], [15].

The incremental-iterative form of the equations for time step Δt and equilibrium iteration "i" are:

$$\begin{bmatrix} \frac{1}{\Delta t} \mathbf{M}_v + {}^{t+\Delta t} \mathbf{K}_{vv}^{(i-1)} + {}^{t+\Delta t} \mathbf{K}_{\mu v}^{(i-1)} + {}^{t+\Delta t} \mathbf{J}_{vv}^{(i-1)} & \mathbf{K}_{vp} \\ \mathbf{K}_{vp}^T & \mathbf{0} \end{bmatrix} \begin{Bmatrix} \Delta \mathbf{v}^{(i)} \\ \Delta \mathbf{p}^{(i)} \end{Bmatrix} = \begin{Bmatrix} {}^{t+\Delta t} \mathbf{F}_v^{(i-1)} \\ {}^{t+\Delta t} \mathbf{F}_p^{(i-1)} \end{Bmatrix} \quad (4)$$

The left upper index “t+Δt” denotes that the quantities are evaluated at the end of time step. The matrix M_v is a mass matrix, K_{vv} and J_{vv} are convective matrices, $K_{\mu v}$ is the viscous matrix, K_{vp} is the pressure matrix, and F_v and F_p are forcing vectors. The pressure is eliminated at the element level through the static condensation. A parallel version of the solver is used. In addition to the velocity field, the wall shear stress computation is performed. The mean shear stress τ_{mean} within a time interval T is calculated as [14]

$$\tau_{mean} = \left| \frac{1}{T} \int_0^T \mathbf{t}_s dt \right| \quad (5)$$

where \mathbf{t}_s is the surface traction vector. Another scalar quantity is a time-averaged magnitude of the surface traction vector, calculated as

$$\tau_{mag} = \frac{1}{T} \int_0^T |\mathbf{t}_s| dt \quad (6)$$

The interface for fluid-structure interaction algorithm is presented in Fig. 7.

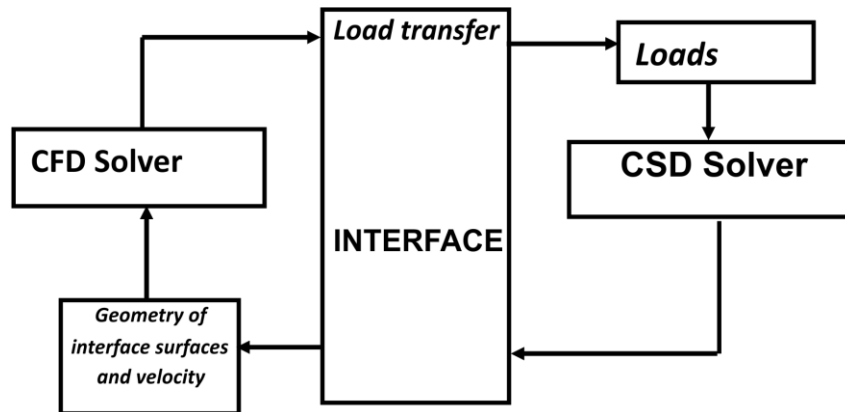


Fig. 7. Information exchange for the coupled problem fluid-structure interaction

We use the loose coupling solution algorithm, ([16]) for the fluid-structure interaction problem. The loose coupling has many advantages with respect to

Modeling of Arterial Stiffness using Variations of Pulse Transit Time

the strong coupling approach. The main goal is to reuse CFD and CSD codes with a minimum of modifications. The fluid and solid variables are updated alternatively by the independent CFD and CSD codes with exchange boundary information at each time step, as it is shown in Fig. 7.

The CFD solver needs the position and the velocity of the interface surface. This information is a part of the solution of the CSD problem. On the other hand, the CSD solver takes the fluid loads on the interface surface from the CFD solver as the boundary conditions and solves for the deformation. The most attractive feature of the loose coupling approach is that the CFD and CSD solvers do not need to be rewritten.

In the initialization phase the master code first reads the necessary input file for the CSD and CFD solvers, initializes the arrays, and identifies the points common for the fluid and solid domains. These points are the ones used for the exchange information between CFD and CSD codes.

The master code drives the solution of the coupled problem. It contains a global loop in which the fluid and structure solvers are called alternatively. Inside the global loop several major operations are: call the CFD solver to advance the fluid solution, transfer the computed loads to the solid, call the CSD solver to update the solid solution, and transfer the interface position to the fluid. The global algorithm of the procedure is shown in Fig. 8 [16].

The finite element mesh discretization of the straight blood vessel is shown in Fig. 9a. For fluid domain we used 3D linear 8-node finite element method with 8 linear velocity shape function and constant pressure per element. Penalty method was implemented in order to reduce time for calculation. For solid domain 3D linear 8-node finite element is used with 8 linear displacement shape function. Linear material model and geometry linear analysis with small deformation is used. The fluid domain is discretized with structured mesh of 7400 fluid nodes and solid domain contains 5600 solid nodes. Blood is taken as an incompressible Newtonian fluid, which is appropriated for the large arteries. The blood density is $\rho=1.025 \text{ g/cm}^3$, and the kinematics viscosity is $\nu=0.035 \text{ cm}^2/\text{s}$ [13].

The contour slice of velocity magnitude and wall shear stress are shown in Figs. 10 and 11 for early flow deceleration $t=0.4 \text{ s}$, in the case of deformable and rigid walls.

The Fig. 10 shows the difference between the velocity of fluid in case of deformable and rigid walls. Deformable walls show lower fluid velocity because greater radial displacement which reduces the speed of the fluid. Distributions of wall shear stress for early flow deceleration ($t=0.4 \text{ s}$) are shown in Fig. 11.

The results for wall shear stress (Fig. 11) show generally lower shear stresses for deformable walls in comparison to the rigid wall. This is due to more continuous changes of the velocities near the walls (smaller velocity gradient) under pulsatility conditions when the walls are considered as deformable media.

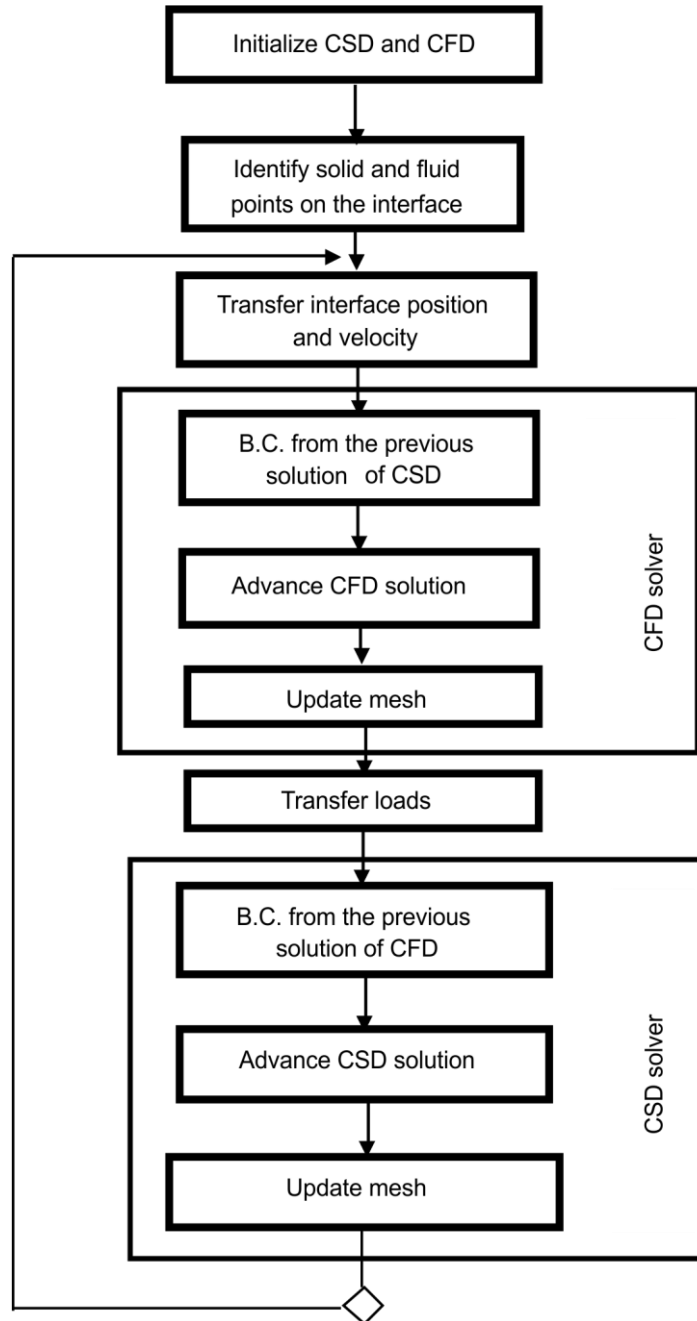
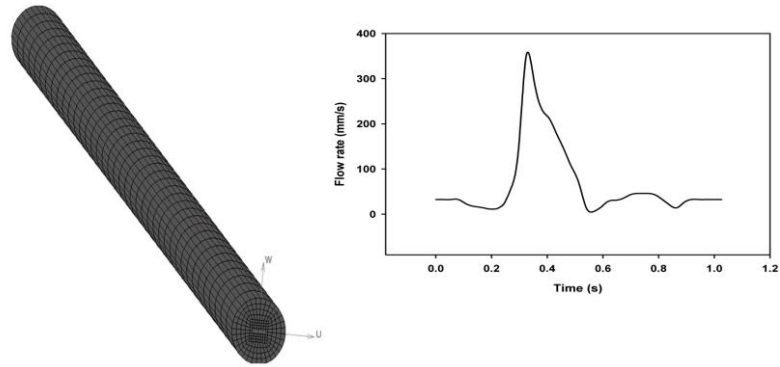


Fig 8. Algorithm for solving fluid-structure problem

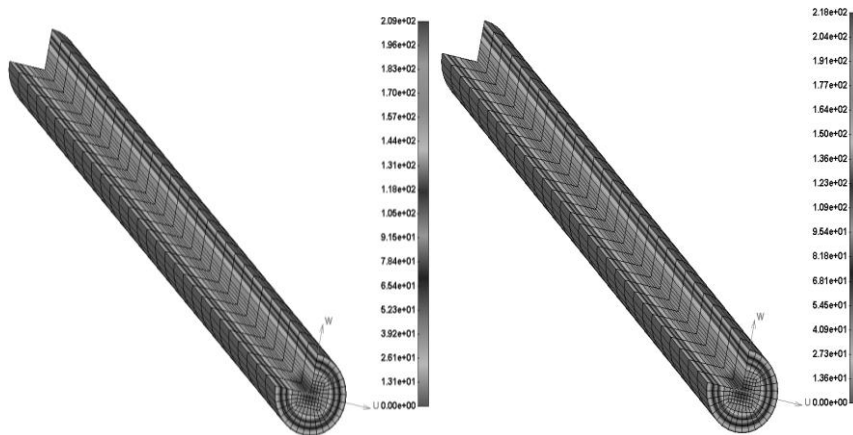
Modeling of Arterial Stiffness using Variations of Pulse Transit Time



a)

b)

Fig. 9. FE model of the blood vessel: a) Finite element mesh; b) Input flow rate vs. time (pulsatile flow)



a)

b)

Fig. 10. The velocity magnitude field in the blood vessel for early deceleration flow $t=0.4$ s: a) Deformable walls; b) Rigid walls

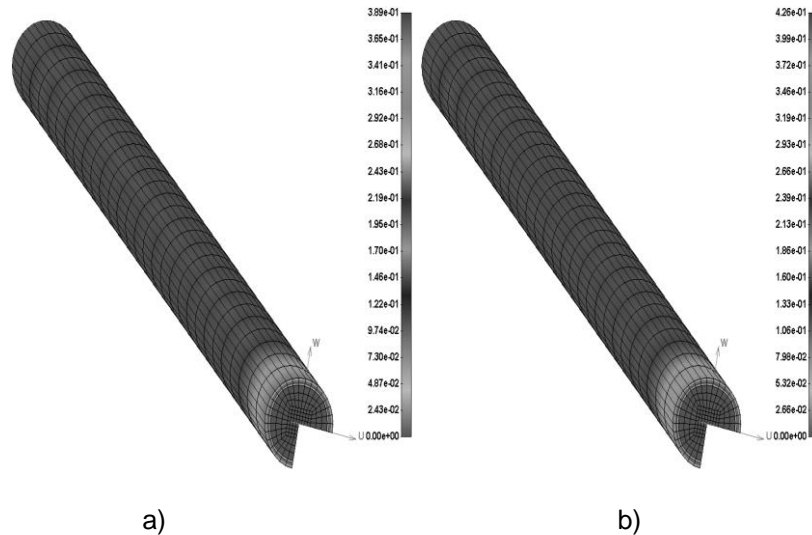


Fig. 11. The wall shear stress in the blood vessel model for early flow deceleration $t=0.4$ s: a) Deformable walls; b) Rigid walls

A great attention was devoted to matching the results obtained from our models with the results obtained by measurements described in the section experimental measurements. In fact, we tried to fit Young's modulus for all different physiological states (experimental breathing protocols), which represent the relationship between PTT signal and pressure.

To fit elasticity modules (for each breathing pattern) we used a simplex optimization method developed by John Nelder and Roger Mead [17]. This method is extremely simple and involves only function evaluations (no derivatives). Function that was minimized is calculated as a sum of eight squared error functions - one for each breathing pattern. These squared error functions represent the difference between measured PTT values and PTT values calculated by substituting modules E in (2).

Each pattern of breathing is simulated by time functions of the flow of fluids. As a result of these input functions, we obtained the corresponding pulse wave velocities that are inserted in PTT formula (3) and get a set of values for the PTT signal. Our task was to fit the module E , so that the calculated PTT signal corresponds to the measured human values. The fitting results are shown in Fig. 12, 13 and 14.

Modeling of Arterial Stiffness using Variations of Pulse Transit Time

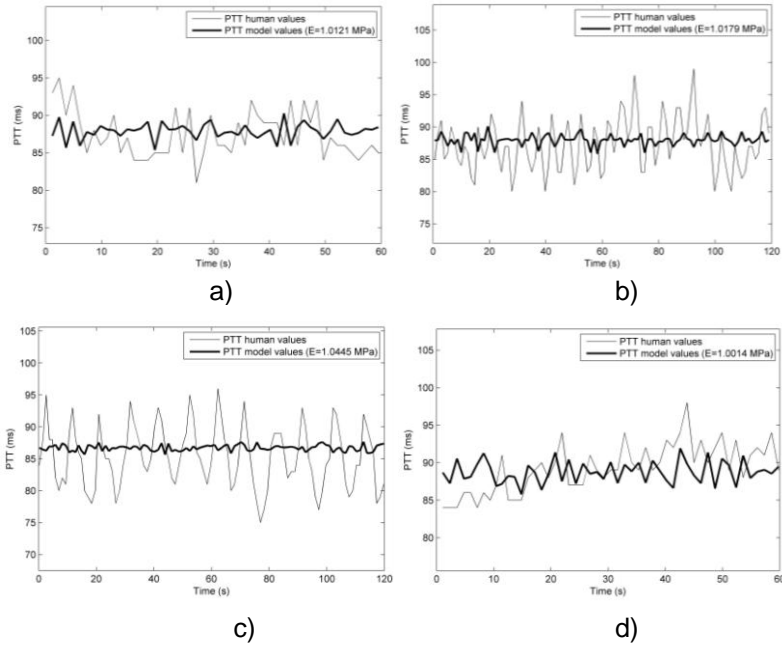


Fig. 12. The fitting results of modules E_1 , E_2 , E_3 and E_4 for Subject_1: a) Fitting result of first pattern breathing; b) Fitting result of second pattern breathing; c) Fitting result of third pattern breathing, d) Fitting result of fourth pattern breathing

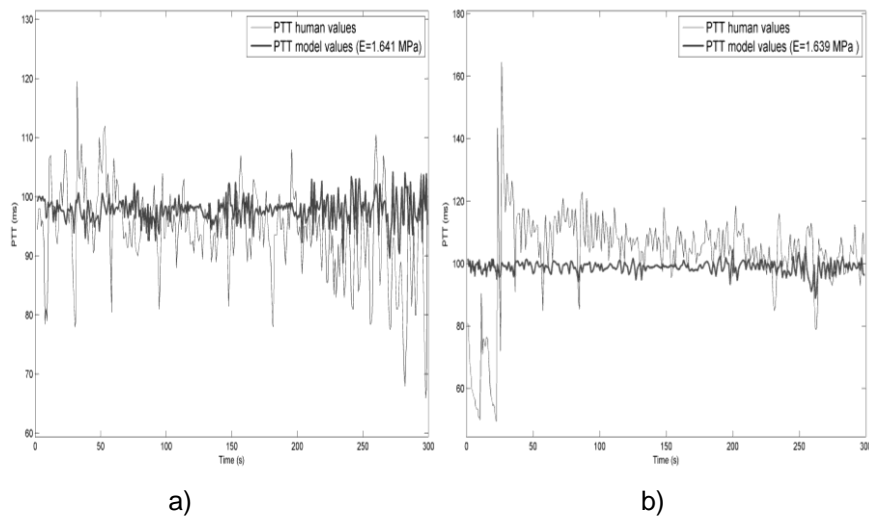


Fig. 13. The fitting results of modules E_5 , E_6 for Subject_2: a) Fitting result of first pattern breathing; b) Fitting result of second pattern breathing

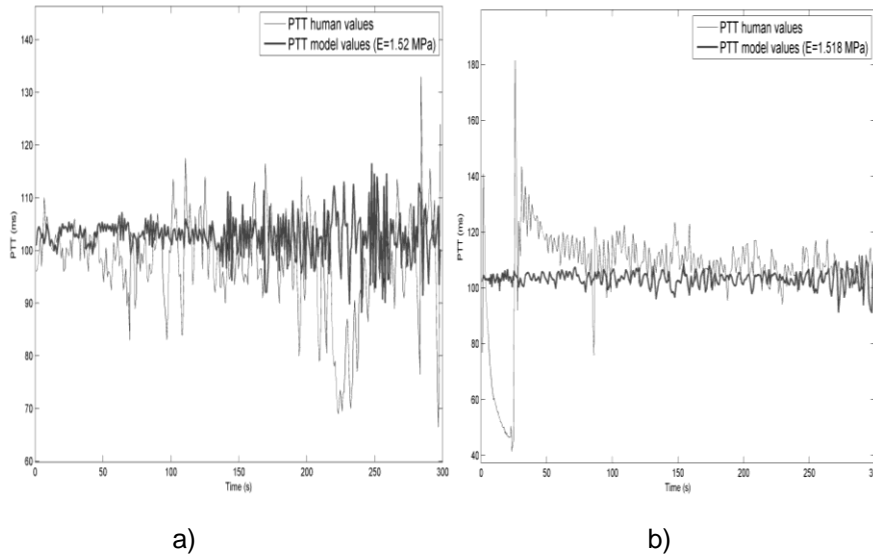


Fig. 14. The fitting results of modules E_7 , E_8 for Subject_3: a) Fitting result of first pattern breathing; b) Fitting result of second pattern breathing

It can be seen from figures 12-14, that for each particular subject with a few pattern breathing it is possible to determine approximately one Young's elasticity module E which is very important for estimation of arterial wall condition. Subject_1 has approximately elasticity module $E=1.02$ MPa, Subject_2 has $E=1.64$ MPa and Subject_3 has $E=1.52$ MPa which are in physiological range of the elasticity modules. Further research is necessary to connect more subject and patient data with PTT measurements, like sex, age, history of disease, blood analysis etc.

5. Discussion and conclusions

The proposed model is simplification of simulation for the complex pulsatile flow through arterial system and non-invasive measurement of PTT. The initial results have shown good correlation and validation for estimation of the arterial stiffness. The assumption of the elastic behavior of the walls is used which is simplification of the nonlinear compliance of the arterial wall. Even with this approximation good results are achieved. Stress distribution inside the wall can be varied with different combination of peripheral resistance, compliance. Also shear stress distribution which is crucial factor for activation of endothelial cells and atherosclerosis disease can be fitted with different change of blood viscosity and concentration of LDL and HDL in the standard blood patient analysis. Using of the administering drugs that alter nitric oxide synthesis in the endothelial cells lining blood vessels can be also easy implemented in this model. Primary aim of this study was to evaluate

Modeling of Arterial Stiffness using Variations of Pulse Transit Time

feasibility of estimation of arterial stiffness using PTT measurements. We measure PTT for different breathing rhythms of the three subjects and compared measurements with simplified finite element fluid-structure interaction model. Numerical simulation analyzed a fluid-structure interaction where fluid and solid domain represent the straight deformable artery segment. The length of numerical model approximately corresponds to the distance from the main aorta root to the finger measurement position of the subject. The simulation results using this simplified approach provide a very good fit with the elastic property of the arterial wall. Therefore, our preliminary results indicate that pulse travel time measurement can be used for noninvasive assessment of the arterial stiffness. We are aware that isotropic assumption of the arterial wall is just first approximation and our future research will go in direction to include more complex component materials. Difference in time-history of measured and simulated PPT values is also due to isotropic assumption of the arterial wall. This is an extension of our work in [18] in terms of more subjects in the experiment and flow-chart for CFD program as well as the algorithm for coupled problem fluid-structure interaction are described in details.

The proposed method could allow the implementation of screening diagnostics. For clinical using it is sufficient to register equal duration of ECG signal and the distal arterial pulse, which are carried out with non-invasive methods by means of widely available monitoring devices.

Acknowledgments. This work has been partly supported by Ministry of Education and Science of Serbia, Grant No. III-41007, OI-174028 and FP7 ICT-2007-2-5.3 (224297) ARTreat project.

References

1. Allen, J.: Photoplethysmography and its application in clinical physiological measurement. *Physiological measurement*, Vol. 28, No. 3. (2007)
2. Cox, P.O., Madsen, C., Ryan, K. L., Convertino, V. A., Jovanov, E.: Investigation of Photoplethysmogram Morphology for the Detection of Hypovolemic States, 30th Annual International IEE EMBS conference, Vancouver, BC. 5486 – 5489. (2008)
3. McDonald, Nichols, W.W., O'Rourke, M.F.: McDonald's blood flow in arteries: theoretical, experimental and clinical principles. Oxford University Press. (1988)
4. Steptoe, A.: Pulse wave velocity and blood pressure changes: calibration and applications. *Psychophysiology*, Vol. 13, 488-493. (1976)
5. Callaghan, F.J., Geddes, LA., Babbs, CF., Bourland, JD.: Relationship between pulse-wave velocity and arterial elasticity. *Med Biol Eng Comp*, Vol. 24, No. 3. 248–254. (1986)
6. Laurent, S., Boutouyrie, P., Asmar, R.: Aortic stiffness is an independent predictor of all-cause and cardiovascular mortality in hypertensive patients. *Hypertension*, Vol. 37. 1236–1241. (2001)
7. Constant, I., Laude, D., Murat, I.: Pulse rate variability is not a surrogate for heart rate variability. *Clinical Science*, Vol. 97. 391–397. (1999)

Aleksandar Peulić et al.

8. Drinnan, M.J.: Relation between heart rate and pulse transit time during paced respiration. *Physiology Measurement*, Vol. 22. 425–432. (2001)
9. Giardino, N.D.: Comparison of finger plethysmograph to ECG in the measurement of heart rate variability. *Psychophysiology*, Vol. 39. 246-252. (2002)
10. Johansson, A.: Estimation of respiratory volumes from the photoplethysmographic signal part.1: experimental results. *Med.Biol.Eng. Comput.*, Vol. 37. 42-47. (1999)
11. <http://www.nonin.com/>
12. Wong, Y.M., Zhang, Y.T., The effects of exercises on the relationship between pulse transit time and arterial blood pressure. *Conf. of IEEE Engineering in Medicine and Biology Society*, Vol. 5 5576-5578. (2005)
13. Filipovic, N., Ivanovic, M., Krstajic, D., Kojic, M.: Hemodynamic flow modeling through an abdominal aorta aneurysm using data mining tools. *IEEE Transactions on Information Technology in BioMedicine*, Vol. 15, No. 2, 189-194. (2011)
14. Filipovic N, Milasinovic D, Zdravkovic N, Böckler D, von Tengg-Kobligk H.: Impact of aortic repair based on flow field computer simulation within the thoracic aorta. *Computer Methods and Programs in Biomedicine*, Vol. 101, No. 3, 243-52. (2011)
15. Kojic M, Filipovic N, Zivkovic M, Slavkovic R, Grujovic N: PAK Finite Element Program. Faculty of Mech. Engrg, University of Kragujevac, Serbia. (2010)
16. Filipovic N., Mijailovic S., Tsuda A. and Kojic M.: An Implicit Algorithm Within The Arbitrary Lagrangian-Eulerian Formulation for Solving Incompressible Fluid Flow With Large Boundary Motions. *Comp. Meth. Appl. Mech. Eng.* Vol 195. 6347-6361. (2006)
17. Nelder, J., Mead, R.: A simplex method for function minimization. *Computer Journal* Vol. 7, No.2, 308-313. (1965)
18. Peulic A., Jovanov, E., Radovic, M., Saveljic, I., Zdravkovic, N. Filipovic, N.: Arterial Stiffness modeling using variations of Pulse Transit Time. 10th BioEng, 5-7 October, Kos, Greece (2011).

Aleksandar Peulić received the Diploma degree in electronic engineering from Faculty of Electronic Engineering, University of Nis, Nis, Serbia, in 1994, the Master of Science in electrical engineering from Faculty of Electronic Engineering, University of Nis, Nis, Serbia, in 2000 and the Ph.D. degree in electrical engineering from the University of Kragujevac, Kragujevac, Serbia, in 2007. From 2005 to 2007, he was part time with the University of Maribor as doctoral research. From 2008 to 2009, he was as postdoctoral at the University of Alabama in Huntsville. His research interests include microcontrollers systems, wearable sensors, bioengineering, software engineering, and computer control systems.

Nataša Milojević graduated at Faculty of Mechanical Engineering, University of Belgrade, Serbia, in 1995. Received the Diploma degree for Master of Science at the same University, in the area of Bioengineering. Currently works on the Ph.D. From 1995 to 1997, worked as assistant at Faculty of Mechanical Engineering, University of Belgrade. From 1997 until

Modeling of Arterial Stiffness using Variations of Pulse Transit Time

now works in the Intellectual Property Office of Serbia as Counselor for patents. Interested in bioengineering, patent searching and process engineering.

Emil Jovanov is an Associate Professor in the Electrical and Computer Engineering Department at the University of Alabama in Huntsville. He received his Dipl. Ing., MSc, and PhD from the University of Belgrade. He is recognized as the originator of the concept of wireless body area networks for health monitoring and he is one of the leaders in the field of wearable health monitoring. His research interests include wearable health monitoring, ubiquitous and mobile computing, and biomedical signal processing

Miloš Radović is PhD student at Faculty of Engineering in University of Kragujevac. His research interests include data mining, medical imaging reconstruction and nonlinear parameter estimation.

Igor Saveljić is PhD student at Faculty of Engineering in University of Kragujevac. His research interests include 3D mesh generation, finite element method, fluid-structure interaction and nonlinear parameter estimation.

Nebojša Zdravković received the Ph.D. in bioengineering from the University of Kragujevac, Serbia in 2000. He is currently a Associate Professor in Informatics and Medical Statistics at Faculty of Medical Science, University of Kragujevac, Serbia His research interests are in data mining, statistical methods, finite element method fluid mechanics, coupled problems

Nenad Filipović received the Ph.D. in bioengineering from the University of Kragujevac, Serbia in 1999. He was Research Associate at Harvard School of Public Health in Boston, USA. He is currently a Professor in Bioengineering at Faculty of Engineering, University of Kragujevac, Serbia. His research interests are in the area of fluid mechanics, coupled problems; fluid-structure interaction, heat transfer; biofluid mechanics; biomechanics, multi-scale modeling, discrete modeling, molecular dynamics, computational chemistry and bioprocess modeling. He is author and co-author 6 textbooks and 1 monograph on English language, over 50 publications in peer review journals and over 5 software for modeling with finite element method and discrete methods from fluid mechanics and multiphysics. He leads a number of national and international projects in area of bioengineering.

Received: May 31, 2012; Accepted: December 18, 2012.

